Electronic Supplementary Material (ESI) for Catalysis Science & Technology.

Supporting Information:

Promotional Role of Additive La on the NO Oxidation Performance of $SmMn_2O_5$ Mullite Catalyst

Zijian Feng[a], Jianqiang Wang[b], Xiao Liu[c], Yanwei Wen[a], Rong Chen[c], Hongfeng Yin[d], Meiqing Shen[b,*], Bin Shan[a,*]

[a]State Key Laboratory of Material Processing and Die and Mould Technology and School of Materials Science and Technology, Huazhong University of Science and Technology, Wuhan 430074, China.

[b]School of Chemical Engineering and Technology, Tianjin University, 92 Weijin Road, Nankai District, Tianjin 300072, China.

[c]State Key Laboratory of Digital Manufacturing Equipment and Technology and School of Mechanical Science and Engineering, Huazhong University of Science and Technology, Wuhan 430074, Hubei, China.

[d]Division of Fuel Cell & Energy Technology, Ningbo Institute of Material Technology and Engineering, Chinese Academy of Sciences, Ningbo 315201, Zhejiang, China.

*Corresponding Author:

Bin Shan, Fax: +86-27-87542857, E-mail: bshan@mail.hust.edu.cn (B. Shan);

Meiqing Shen, Fax: +86-22-27407002, Email: mqshen@tju.edu.cn (M. Q. Shen).

S1. Mass diffusion effect

Here, the LSM3 catalyst (25 mg) with the highest NO conversion is used as an example to rule out the diffusion limitations. In order to rule out the external mass transfer limitation, ten space velocities (SVs) had been used. Fig. S1 presents the variation in NO conversion rate as a function of SV (1.2 – 21.6×10^5 ml/(g • h)) at 270°C. As shown in Fig. S1, the rate of NO conversion initially increased with the increasing space velocity and then remained unchanged at SV >9.6×10^5 ml/(g • h). It is indicated that the NO conversion rate was not affected by the external mass transfer limitation when the SV was higher than 9.6×10^5 ml/(g • h). We had chosen the condition with SV = 9.6×10^5 ml/(g • h) to ensure that the reaction is free from external mass transfer limitation. Furthermore, this point was repeated at the end of this series of experiments (Red Solid).

We examined the internal mass transfer limitation by measuring the rates using the sample with four different particle sizes at 270°C, see Fig. S2. For the sample with three particle diameters within the range of 100 - 180 μm, the measured rates were almost constant, indicating the NO conversion rates of the sample with particle sizes in this range could not be affected by the internal mass transfer. The sample with 150 - 180 μm diameter (80~100 mesh) was tested twice to confirm the stability and accuracy (Red Solid).

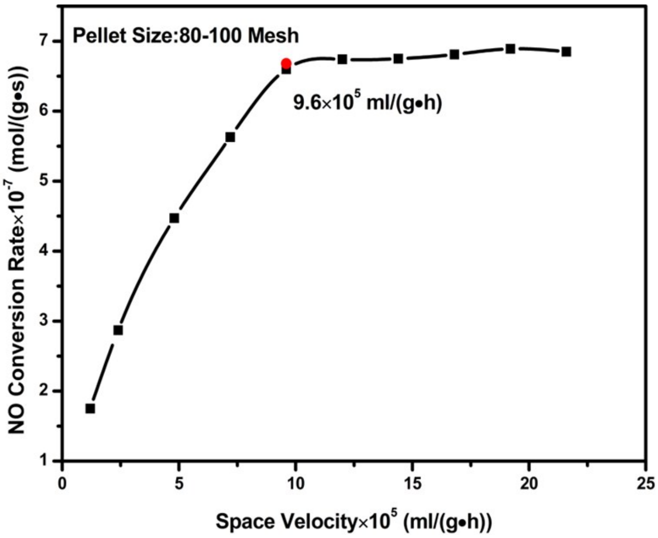

Fig.S1 NO conversion rate of LSM3 catalyst for NO oxidation reaction as a function of SV/(ml/(g·h)) at 270°C. Red solid is the duplicated point at SV = 9.6×10^5 ml/(g·h)

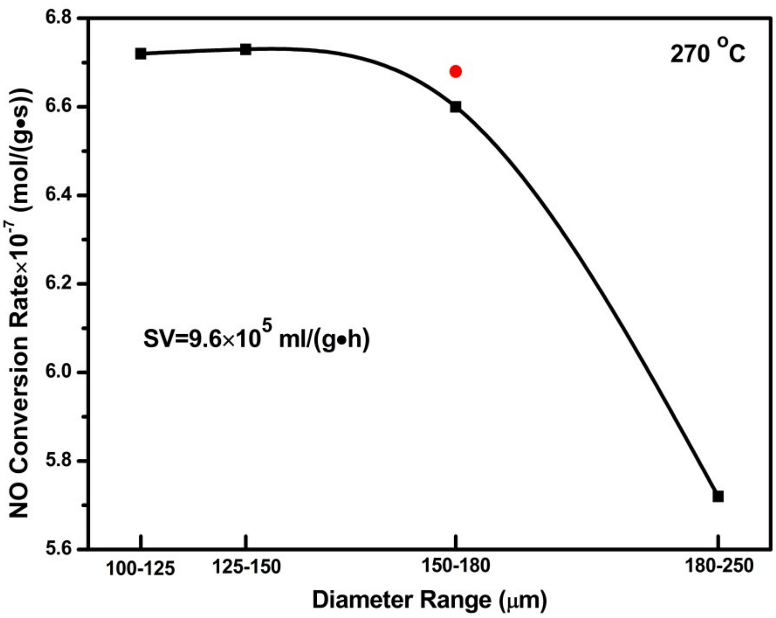

Fig.S2 NO conversion rate of LSM3 catalyst for NO oxidation reaction as a function of particle size at 270°C. Red solid is the duplicated point at 80 - 100 mesh

S2. Inhibition effect of NO_2 on NO oxidation reaction over $La_{0.3}Sm_{0.7}Mn_2O_\delta$ catalyst

The inhibition effect of NO_2 on the NO oxidation reaction over La modified mullite catalysts was examined by introducing various amounts of NO_2 fed into the feed stream. Fig. S3 shows the alteration of NO_2 production with respect to the total concentration of NO_2 (NO_2 produced by oxidation + NO_2 introduced) in the reaction temperature range from 180 to 240 °C. Although NO_2 was added into the feed gas stream, the conversion of NO to NO_2 over $La_{0.3}Sm_{0.7}Mn_2O_\delta$ remained constant when the total concentration of NO_2 was around 60 ppm, and began to decrease until the total concentration of NO_2 reached to 80 ppm, regardless of the reaction temperature. This result indicated that the inhibition of NO oxidation reaction by NO_2 produced was negligible at low conversion levels below 20%, based on the feed concentration of 400 ppm NO. Thus in order to minimize the inhibition effect, we kept the conversion below 15% for kinetic analysis and the temperature range was 160-220 °C.

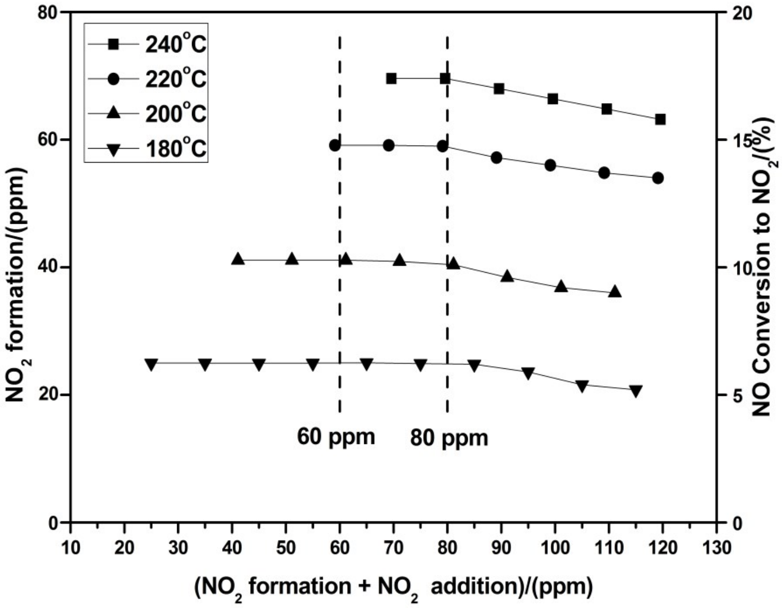

Fig. S3 Inhibition of NO_2 on NO oxidation reaction over $La_{0.3}Sm_{0.7}Mn_2O_\delta$. Feed: 400 ppm NO, 0 to 90 ppm NO_2, 10% O_2 and N_2 balance. Flow rate: 400 ml/min

S3. Catalytic performance of individual oxide

Fig. S4 presents the conversions of NO as a function of the reaction temperature over the pure $SmMn_2O_5$ mullite, Mn-rich non-stoichiometric perovskite $La_{0.96}MnO_{3.05}$ (calcined at 700 ^{o}C and 800 ^{o}C, respectively), Mn_3O_4 and La_2O_3. From the results we can see that the Mn-rich perovskite got worse catalytic property for NO oxidation than that of mullite through the whole temperature range. Mn_3O_4 showed activity only above 300 ^{o}C with the highest conversion of 12%, and La_2O_3 didn't even show any activity, these two oxides may not contribute much with low content and poor catalytic performance. All these results indicated a synergetic effect existing between the mullite and perovskite promoted the catalytic activity in La modified multiphase catalysts.

The BET surface area of $La_{0.96}MnO_{3.05}$ was 18.31 m^2/g for 700 ^{o}C calcined sample and 6.79 m^2/g for 800 ^{o}C calcined sample, and the surface area of $SmMn_2O_5$ was 15.70 m^2/g. The NO oxidation catalytic activity of mullite and perovskite were compared on the basis of surface area. The reaction rates ($\mu mol\cdot s^{-1}\cdot m^{-2}$) through 200-300 ^{o}C were listed in Table S1. From the results, we can see that for $La_{0.96}MnO_{3.05}$, the reaction rates of 700 ^{o}C calcined sample were lower than 800 ^{o}C calcined sample and mullite through the whole temperature range due to the larger surface area. Note that the multiphase catalysts were calcined at 800 ^{o}C for 8 hours, it is more reasonable to compare the reaction rates of 800 °C calcined perovskite with mullite on the basis of surface area. From Table S1, we can see that the reaction rates of mullite were higher than perovskite at temperatures below 275 °C, while lower than perovskite at temperatures higher than 275 °C. The results indicated that the catalytically active site for low temperature NO oxidation was mainly mullite phase, the non-stoichiometric perovskite resulted in additional high-temperature (>300 °C) catalytic activity.

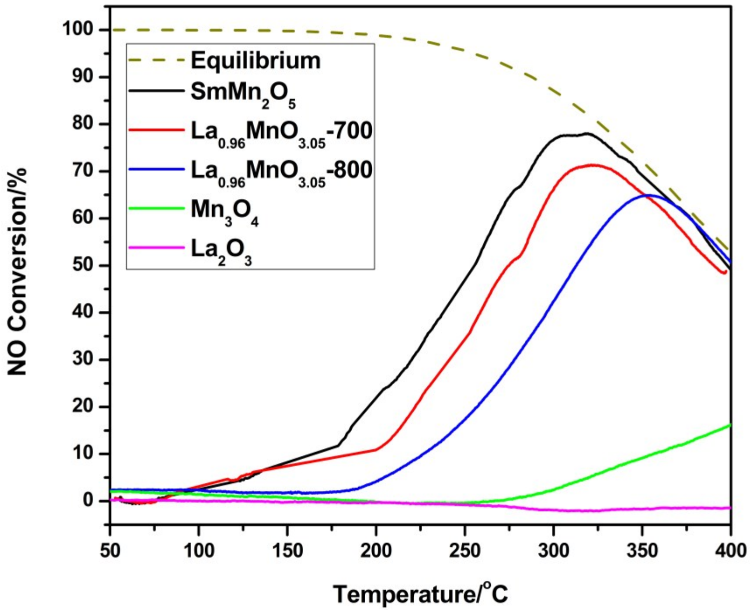

Fig. S4 Activities of fresh mullite $SmMn_2O_5$, perovskite $La_{0.96}MnO_{3.05}$ (700 °C and 800 °C calcined, respectively), Mn_3O_4, La_2O_3 for NO oxidation. Feed: 400 ppm NO, 10% O_2, 3% H_2O and N_2 as balance

Table S1 NO oxidation rates on the basis of surface area of mullite and perovskite.

Temperature (°C)		200	225	250	275	300
Reaction Rates (10^{-2} μmol·s^{-1}·m^{-2})	$SmMn_2O_5$	0.78	1.03	1.49	1.83	2.08
	$La_{0.96}MnO_{3.05}$ (700 °C)	0.31	0.59	0.91	1.22	1.54
	$La_{0.96}MnO_{3.05}$ (800 °C)	0.33	0.69	1.19	1.85	2.48

S4. Effect of H_2O on NO oxidation activity of $La_xSm_{1-x}Mn_2O_\delta$ (x=0, 0.3)

NO oxidation activity of $La_xSm_{1-x}Mn_2O_\delta$ (x = 0, 0.3) was evaluated with the feed gas stream containing 400 ppm NO, 10% O_2, 0 or 3% H_2O and N_2 balance with total flow rate of 600 ml/min.

As shown in Fig. S5, the NO oxidation performance of $La_xSm_{1-x}Mn_2O_\delta$ was inhibited by the presence of H_2O for both x = 0 and 0.3, particularly at low temperatures below 300 °C. However, $La_{0.3}Sm_{0.7}Mn_2O_\delta$ still exhibited a much higher NO oxidation activity than $SmMn_2O_5$, with or without H_2O in the feed stream. And $La_{0.3}Sm_{0.7}Mn_2O_\delta$ obtained a maximum conversion of 91% at about 255 °C, lower than reported mixed phase oxides $SmSrCeMn_7O_{14.83}$, which showed a maximum conversion of 90% at about 320 °C. [1]

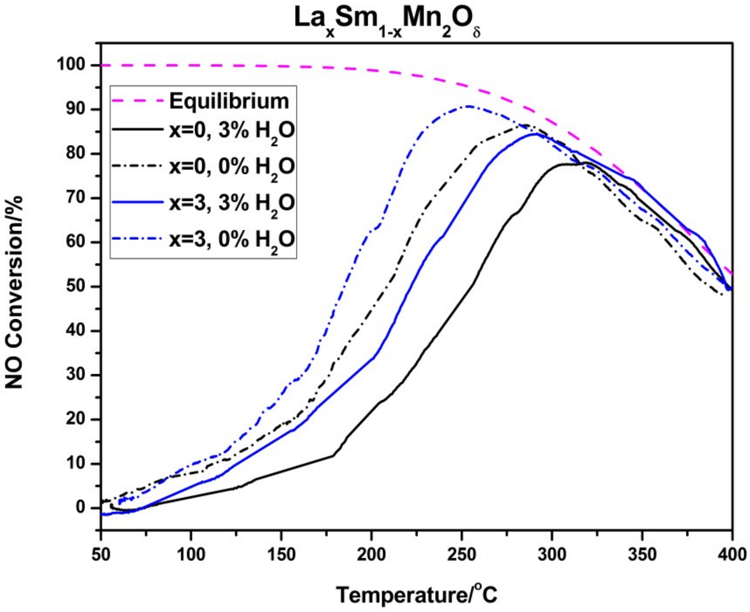

Fig. S5 Effect of H_2O on NO oxidation activity over $La_xSm_{1-x}Mn_2O_\delta$ (x=0, 0.3). Feed: 400 ppm NO, 10% O_2, 0 or 3% H_2O and N_2 balance

S5. NO adsorption behavior

The adsorption and desorption capability of NO is an important factor influencing the catalytic performance. The NO desorption behavior is shown in Fig. S6. There were two main desorption peaks in the whole temperature range, one below 200 °C and the other close to 300 °C. A small peak appeared between 200 °C and 250 °C for LSM3 and LSM5 samples, which might be due to stronger NO physisorption on the samples. The desorption species below 200 °C could be the nitrogen-containing species desorbed from active sites. Above 250 °C the detected NO could be attributed to the decomposed metal nitro or nitrate on the catalysts surface. The total NO adsorption amount was summarized in table S2. Generally, it is considered that there is a positive correlation between total NO adsorption amount and BET results, for higher BET surface area could lead to more adsorbing sites and reaction active sites. Thus more amount of NO adsorbed on the surface sites of LSM5 and LSM3 than that of LSM0 and LSM1 catalysts with LSM1 obtaining least amount of adsorbed NO, consistent with BET results. As for the LSM3 catalyst, the first desorption peak shifted to lower temperature by a 70 ^{o}C, which meant that the adsorbed NO on LSM3 was easier to break up to react with active oxygen, indicating higher activity of LSM3 towards NO oxidation at temperature below 150 ^{o}C. However, the LSM5 which got the highest amount of desorption NO had a lower activity than the LSM3. The results indicated that the catalytic activities of samples are not simply determined by absorbed NO amount and desorption behavior.

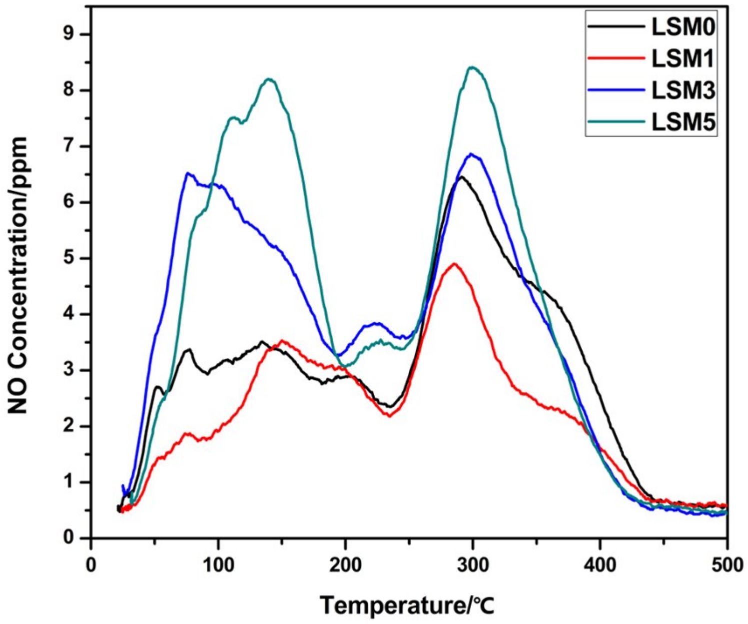

Fig. S6 NO-TPD profile over fresh LSM samples

Table S2 NO adsorption amount of $La_xSm_{1-x}Mn_2O_\delta$, x=0, 0.1, 0.3, 0.5.

$La_xSm_{1-x}Mn_2O_\delta$		x=0	x=0.1	x=0.3	x=0.5
adsorption amount (μmol/g)	0-250 ^{o}C	10.59	8.75	17.35	18.56
	250-400 ^{o}C	12.28	8.47	10.88	12.35

S6. DRIFTS study of $La_xSm_{1-x}Mn_2O_\delta$ with various temperatures

DRIFTS study of $La_xSm_{1-x}Mn_2O_\delta$ at 150 ^{o}C and 300 ^{o}C in $NO+O_2$ atmosphere. To more concretely determining the effect of La content on site specific reactivity, the IR spectra of $NO+O_2$

for the $La_xSm_{1-x}Mn_2O_\delta$ (x=0, 0.1, 0.3, 0.5) samples at different temperatures were evaluated as shown in Fig. S7. All the key reaction intermediates in the oxidation of NO to NO_2 decreased with temperature increase. However, the decrease of the intensity of main reaction intermediates for various catalysts was different. Taking Mn bi-dentate nitrate located at 1571 cm^{-1} as as an example, the loss of the intensity is 51% for x=0, 53.5% for x=0.1, 64.5% for x=0.3 and 61.4% for x=0.5, a higher percent of decrease generally indicated an easier conversion of reaction intermediate to NO_2 formation, and better specific cite reactivity.

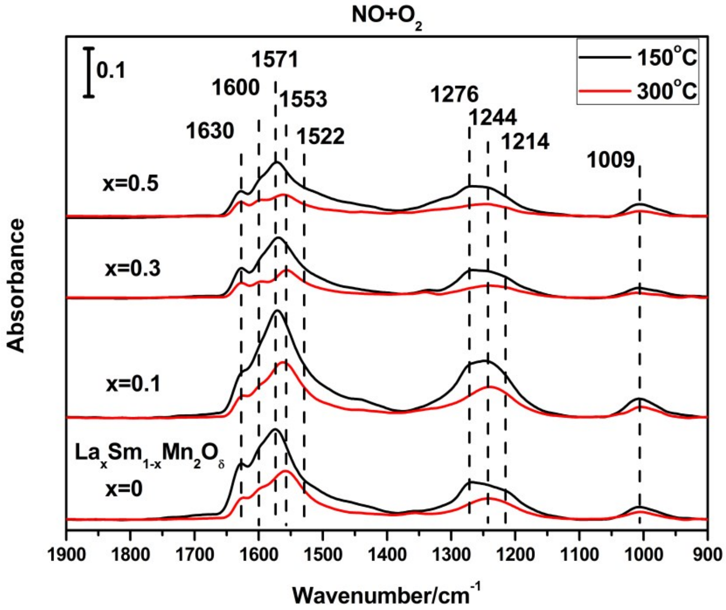

Mn bi-dentate nitrate: 1630 and 1571 cm^{-1}; Mn mono-dentate nitrate: 1522 and 1276 cm^{-1};
Mn bridged nitrate: 1214, 1244 and 1009 cm^{-1}; Mn mono-dentate nitrite: 1600 cm^{-1};
Sm nitrate: 1553 cm^{-1}; La_2O_3 NO chelating: 1340 cm^{-1}

Fig. S7 Evolution of DRIFTS spectra at 150 °C and 300 °C on $La_xSm_{1-x}Mn_2O_\delta$ (x=0, 0.1, 0.3, 0.5) samples during exposure to $NO+O_2$ feed gases. Feed: 400 ppm NO, 10% O_2 and N_2 as balance

S7. TEM image of 2 wt.% Pt on γ-Al_2O_3

TEM was employed to examine the Pt nanoparticle, the result is shown in Fig. S8, the particles were well dispersed and the particle size of Pt was around 2-4 nm.

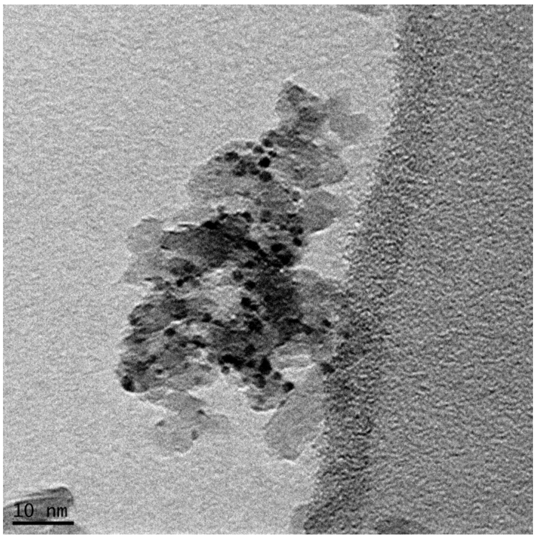

Fig. S8 TEM image of 2 wt.% Pt/Al_2O

Notes and references

1 W. C. Wang, G. McCool, N. Kapur, G. Yuan, B. Shan, M. Nguyen, U. M. Graham, B. H. Davis, G. Jacobs, K. Cho and X. H. Hao, *Science*, 2012, **337**, 832-835.